INTERNATIONAL JOURNAL OF PRECISION ENGINEERING AND MANUFACTURING-GREEN TECHNOLOGY Vol. 3, No. 3, pp. 311-321 JULY 2016 / 311
DOI: 10.1007/s40684-016-0040-4 ISSN 2288-6206 (Print) / ISSN 2198-0810 (Online)

Structural Health Monitoring of Carbon-Material-Reinforced Polymers Using Electrical Resistance Measurement

Hyung Doh Roh[1], Homin Lee[1], and Young-Bin Park[1,#]

1 Department of Mechanical Engineering, Ulsan National Institute of Science and Technology, 50, UNIST-gil, Eonyand-eup, Ulju-gun, Ulsan, 44919, South Korea
Corresponding Author / Email: ypark@unist.ac.kr, TEL: +82-52-217-2314, FAX: +82-52-217-2409

KEYWORDS: Structural health monitoring, Carbon fiber, Carbon nanotube, Composite, Piezoresistivity

This paper presents a review of structural health monitoring techniques for carbon-based materials and structures. Based on the piezoresistivity of carbon, elastic deformation and the failure of carbon structures are visible by monitoring the electrical resistance. Carbon structures have an in-situ real-time self-sensing capability, eliminating the need for additional sensors. Numerous researchers have investigated the electromechanical properties of carbon materials by conducting experiments, numerical analyses, and simulations. In addition, the electrical conductivity of carbon is reinterpreted as an electrically equivalent circuit in order to investigate orientation-dependent sensing.

Manuscript received: June 5, 2016 / Revised: June 25, 2016 / Accepted: June 30, 2016 (Invited Paper)

1. Introduction

As more and more large structures, such as buildings, bridges, and aircraft, are constructed and at the same time existing structures are being aged, ensuring their structural integrity and safety is becoming more important. In 1995, the Sampoong Department Store in Seoul, South Korea, collapsed resulting in more than 500 deaths. The financial damage and number of casualties were so great that the entire nation was shocked. Similarly, an interstate bridge collapsed in Oklahoma, U.S., in 2002 resulting in 14 deaths. The safety of a structure must be thoroughly monitored to predict and prevent disasters, which necessitates structural health monitoring (SHM). If SHM had been conducted in advance, such accidents shown in Fig. 1 could have been prevented. Due to a lack of an efficient monitoring system, only a few people were aware of the danger. Thus, we must fully understand and develop effective sensing methods for structures.

Fig. 1 Collapses of Sampoong Department Store, Korea (Left) and I-40 Mississippi River Bridge, U.S. (Right)

Carbon-based materials have received much attention and have replaced steel owing to their light weight and excellent mechanical, thermal, and electrical properties. Subsequently, monitoring the health of carbon structures has emerged as a hot issue with regard to safety.[1-6] This article deals mainly with carbon-SHM technologies.

2. Current SHM Methodologies

SHM tests are classified into two types: schedule-based and condition-based. In addition, some researchers use the terms destructive evaluation and nondestructive evaluation (NDE). Because preserving the safety of the structures themselves is more important, this article deals only with NDE.[7-10] Examples of schedule-based and real-time monitoring are presented below.

The basic level of health monitoring is a visual inspection. To detect microcracks that cannot be observed by the human eye, the eddy current method was adopted.[11-14] Based on Faraday's law of induction, the loops of electric current induced within conductors serve as the medium for this method. When the loop makes contact with a crack, its

shape is changed. However, a critical limitation is its limited sensing range, which is just below the device. This can be a fatal disadvantage when dealing with large structures.

Ultrasonic inspection is a more scientific method for observing defects inside structures.[15-20] An ultrasonic energy pulse is emitted into the structure, and the reflected signal is analyzed by a method called C-scan. The defect size and position are drawn on a 2D display, as shown in Fig. 2(a), based on the time and the amplitude of the travel pulse.[21-24]

The two aforementioned methods are schedule-based inspections that have disadvantages such as being laborious, time wasting, costly, and ineffective. Critically, blind spots between inspection periods are inevitable limitations. The following paragraphs discuss real-time inspections that monitor the structures throughout their life spans.

A PZT (Lead Zirconate Titanate) sensor to which the piezoelectric effect is applied can be utilized as a condition-based sensor for real-time monitoring. When a transmitter transduces a signal, the piezoelectric receiver compares a reference signal with the received signal. If there is a failure, the structure's natural frequency and phase are changed, and a PZT sensor alerts to a failure.[25-29] This method is widely used in aircraft because of its sensitivity (5.0 V/$\mu\varepsilon$). Despite this advantage, this method needs extra devices with corresponding data-channeling sets, and the complexity of the structure increases with the number of devices.

Another state-of-the-art health monitoring technology is a Fiber Bragg Grating (FBG).[30-32] Optical fiber constructed of transparent cores with different and refractive indices penetrates the entire wavelength from a light source as a default. However, when the optical fiber sensor is deformed, some specific wavelengths are reflected, while others pass without any filtration.[33] This, schematically described in Fig. 2(b), can be sensitive to a resolution as small as 2 nm.[34-38] However, it has severe limitations such as high cost and complicated installation requirements. In addition, the FBG is so fragile that its curvature is limited because it is made of glass. The glass causes cladding, which is directly related to poor maintenance resulting from light scattering.

As the sizes of structures have grown, the need for large-area detection methods have increased. Because the applicable range of a single sensor is limited, array types have been adopted to cover entire structures[33,39-42] in various fields with wireless strain gauges, PZTs, and so on. An FBG array[32,37,43] is a representative method to meet the needs of large-structure sensing. The array sensor demerges the structure based on the devices, and monitors the structure section by section, as shown in Fig. 2(c).

When the array form was developed, hybrid sensors in arrays were also suggested, e.g., an acoustic transducer and PZT receivers. The acoustic wave is generated at the center of the actuator and is transmitted to the sensors, as shown in Fig. 2(d).[44] By comparing the phases and natural frequencies of the reference signal and the signal transmitted from the PZT receiver, the location of a crack can be determined.

As explained above, array-formed sensors can enlarge sensing coverage. However, as the number of elements increases, device complexities such as wiring and data handling also increase. Thus, a real-time in-situ sensor that has lower complexity is desperately required.

3. SHM Using Carbon-Based Materials

3.1 Carbon-Based Materials

Carbon has a unique characteristic in that it can combine with other

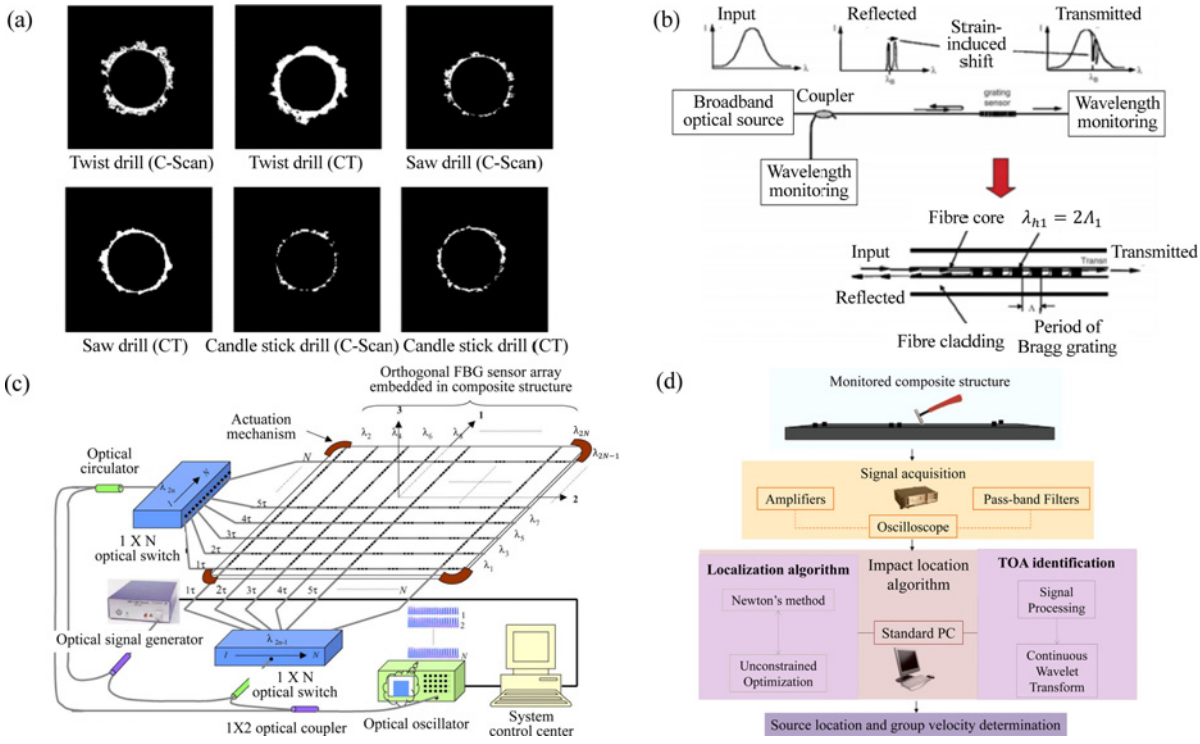

Fig. 2 (a) C-Scan observation of composites from,[23] (b) Principle of FBG from,[33] (c) FBG array measuring the strain of a plate from,[43] (d) Principle of Lamb wave monitoring using PZT receiver from[44] (Adapted from Ref. 23, 33, 43, 44 with Permission)

atoms because there are four electrons in the outer electron shell. Therefore, it can make more than 2000 compounds and has many allotropes with different material properties such as diamond, graphite, fullerene, graphene, CNTs (Carbon Nano-Tubes), and carbon fiber. Diamond and graphite are natural allotropes, but fullerene (1985), CNT (1991), and graphene (2004) (Shown in Fig. 3) and carbon fiber (1969)[45] are synthesized allotropes. Fullerene is composed of 60 carbon atoms in the shape of a soccer ball. Carbon nanotube (CNT) looks like a tube, and graphene resembles a flat sheet. Carbon fiber is the only macroscale substance among them. It is a fiber-type carbon material composed of a graphite crystal structure arranged in a turbostratic fashion. Carbon fiber consists of more than 90% carbon content by weight.

Characteristics of carbon fiber include its high chemical corrosion resistance as well as highly compatible physical properties to weight ratios than those of steel. In addition, it has a negative coefficient of linear expansion ($-0.7 - -1.2 \times 10^{-6}/K$), and high electrical and thermal conductivity.

There are three types of carbon fiber: PAN-based, pitch-based, and rayon-based. These are classified by which base material is used as a precursor. The PAN-based carbon fiber, whose precursor is poly-acrylonitrile, is the most widely used one; it is applicable to the aerospace industry owing to its high tensile strength and shear strength. Pitch-based carbon fiber is based on petroleum, and has a wide elastic modulus range and high thermal and electrical conductivity. Moreover, it is commonly cheaper than PAN-based fiber. Rayon-based carbon fiber, made from regenerated cellulose, is the earliest type among the three. Its applications include nozzles and insulation materials for aerospace industry. However, it lost competitiveness in both performance and cost, making it uncommercializable, because PAN- and pitch-based carbon fibers could be produced and supplied at reasonable costs.

Carbon fibers are also classified as Low Modulus (LM), Intermediate Modulus (IM), High Modulus (HM), or Ultra High Modulus (UHM). LM has material properties with 1000 MPa and 100 GPa. LM is a widely used carbon fiber and other types are called high performance grade carbon fiber.

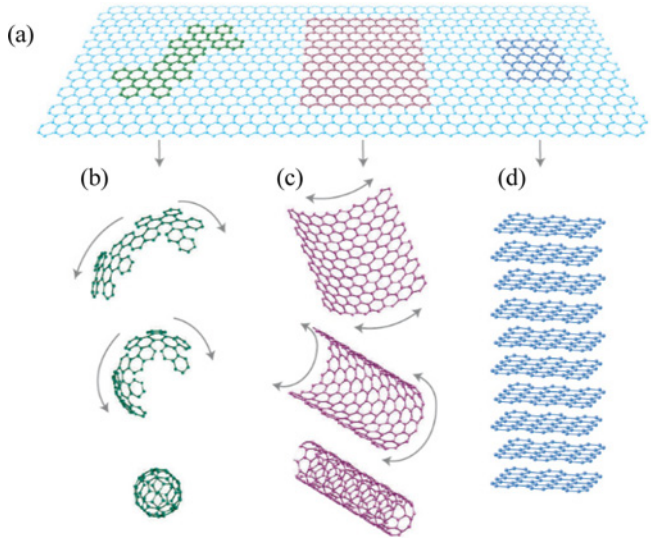

Fig. 3 Allotropes of carbon element: (a) Graphene, (b) Fullerene, (c) Carbon nanotube, (d) Graphite form[45] (Adapted from Ref. 45 with Permission)

Another classification is based on shape: filament, tow, chopped or milled, and fabric. The initial shape of the carbon fiber is a filament with a diameter of 5 to 7 μm, and the tow consists of the gathered filament. The tow can be used as a part of the reinforcement and can be either chopped or milled. Chopped fiber and milled fiber are similar in that both are cut materials, but milled fiber is shorter than chopped fiber. In addition, if it is not cut, the tow can be woven into the fabric as plain-woven, twill, satin, and so on.

There are many advantages to using carbon-fiber-reinforced composites rather than existing structural materials. Physical properties of the composites are superior owing to reinforcing materials that have reduced weight. This is the prominent advantage compared with steel.[46] For this reason, CFRP (Carbon Fiber Reinforced Plastic) can replace steel in various fields. Because energy efficiency is a critical issue in the transportation industry, CFRPs have received much attention, and many companies have adopted carbon fiber composites as structural materials. CFRP is able to reduce the weight sustaining the strength, and hence increase the energy efficiency. For instance, the energy efficiency of the Boeing 787 aircraft increased by 20% due to 60 weight percent of the CFRP use in aircraft.

In addition, another characteristic of CFRP is its electrical conductivity.[47,48] While carbon fiber is highly electrically conductive, the matrix used is so insulative that the electrical directionality reflects the fiber orientation. This is the difference between orthogonal CFRPs and isotropic steel.

The matrix, resin, is classified as either thermoset or thermoplastic. Whereas thermoset cannot return to its original state after curing, thermoplastic can be reshaped above its processing temperature. The reason that thermoset remelting is irreversible is that its curing process contains cross-linking. However, bonding between the polymer chains of thermoplastic is the secondary bonding such as intermolecular forces as weak as melting back is available. This is the critical difference between the thermoset and thermoplastic matrices.

Although thermoset CFRP has a high modulus and high chemical and thermal resistance, it has critical limitations. It cannot be recycled after curing, as previously mentioned, and takes a long time to manufacture, which limits its productivity. These are the reasons why thermoplastic CFRP is actively studied even though thermoset plastic is more dominant in the current marketplace.

3.2 Discontinuous Carbon-Material-Reinforced Polymers

3.2.1 SHM in Elastic Regime

X. Wang, D. D. L. Chung, and their research group are the pioneers of discontinuous carbon-nano-based composite sensing. In 1995, CNT composites were analyzed by compression and tensile tests.[49] Piezoresistive trends were reported as positive piezoresistivity under tension, and negative under compression. This meant that the resistance was proportional to the mechanical strain. The researchers also investigated reinforced cement.[50-53] Cement reinforced by short carbon fiber was studied based on its piezoresistivity. Gauge factors of short-carbon-fiber-reinforced cement were calculated under compressive and tensile tests. One of the studies reported a gauge factor of up to 700 caused by contact resistance.[52]

S. Wen and D. D. L. Chung[54] conducted a comparison analysis of the

reinforcement. Discontinuous carbon fiber and carbon black were discussed in the paper, which concluded that both reinforcing materials enhance the storage modulus but lower the electrical resistance. In addition, the researchers showed the possibility of EMI (Electromagnetic Interference) shielding as well as the softening temperature rise.

J.-M. Park et al.[55] showed apparent progress in CNT composites. They figured out a self-sensing mechanism of carbon fiber and CNT-epoxy composites with the aid of an electromicromechanical technique and acoustic emission. They showed a stress, strain, and electrical resistivity curve in terms of different CNT-dispersed composites. This is shown in Fig. 4. Moreover, a higher modulus of CNT-epoxy composites was procured in this study, owing to enhanced interfacial adhesion and better stress transfer that resulted from choosing an appropriate solution for high-quality CNT dispersion. In addition, Alamusi et al.[56] investigated the piezoresistivity of CNT composites in earnest via both experimental and theoretical analyses.

Furthermore, an electrical-resistance equivalent circuit of CNT composites was created in a study by I. Kang et al..[57] Interestingly, they adopted an electrical resistor-capacitor model that represented strain-dependent CNT networks. Based on a sensitivity analysis with respect to CNT concentrations, neuron sensors for large strains as well as cracking were suggested.

3.2.2 Failure Analysis

In 2002, A. Todoroki et al.[58] published a paper about the delamination identification of cross-ply graphite/epoxy composite beams. Based on electrical resistance changes, the location as well as the size of the delamination could be detected. In accordance with this research, the precision of detecting delamination is determined by selecting an adequate location and by the number of electrodes used.

P. Feraboli et al.[59] conducted various tests such as C-scan, pulsed thermography analysis, and pulse-echo ultrasonic imaging within a molded panel. They discussed inaccuracies in the nondestructive evaluation of composites. However, using piezoresistivity, J. J. Ku-Herrera and F. Aviles[60] verified the self-sensing capability of CNT composites. They conducted cyclic compression tests and mated the electrical resistance and the stress curves with respect to the mechanical strain. They concluded that the electrical resistance catches up the mechanical behavior of the CNT composites.

L. Boger et al. [61] infused epoxy mixed with reinforcing materials into glass fiber. Electrical resistance changes in composites with

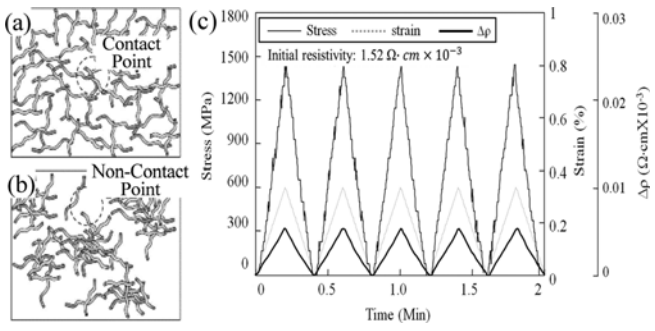

Fig. 4 Schematics comparing (a) Good dispersion and (b) Poor dispersion of CNTs, (c) Results of the cyclic tensile test from[55] (Adapted from Ref. 55 with Permission)

different CNTs and carbon blacks were compared during tensile tests. The ILSS (Interlaminar Shear Strength) of the composite was measured, and a stress/strain analysis and damage monitoring were conducted. Similarly, N. D. Alexopoulus et al.[62] used CNT on glass-fiber-reinforced plastics. His conclusion was that the electrical resistance is correlated with composite damage, and correlation parameters such as resistance, stress, and strain should be changed according to the loading history of the material.

Fatigue tests of CNT composites were studied by A. Vavouliotis et al..[63] The electromechanical response as a damage index under fatigue loading was explored, and the characteristic damage state (CDS) was similar to electrical resistance changes in composites.

J. L. Abot et al.[64] suggested the new idea of using a CNT thread sensor to monitor the strain, damage, and delamination of composite materials. CNT forests were spun into a thread and embedded inside the composites. An integrated sensor monitored strain and damage by electrical resistance changes. During tensile and compressive loading, changes in electrical resistance were used as criteria for deflection, and the differences in residual electrical resistance indicated internal damage of the composites.

3.3 Continuous CFRP Failure and SHM

3.3.1 Types of Failure

Carbon-fiber-reinforced plastic is, literally, a plastic reinforced with carbon fiber. The location of a broken site decides the type of failure.

Fiber pull-out occurs, as the term indicates, when a broken fiber is pulled out from the matrix. This is a result of weakness of the interphase, which is the intermediate section between the reinforcement and the matrix. To prevent fiber pull-out, the interfacial bonding must be enhanced.

A weak bonding strength at the interface, between two different materials, also leads to debonding between the matrix and the fiber. When the reinforcement is separated from the matrix, the composite cannot endure high loads. The same result occurs when using pure resin. Therefore, sustaining the adhesion between the fiber and the matrix without debonding is important for fiber-reinforced plastics.

Fiber rupture and matrix rupture are failures in the fiber and the matrix, respectively. These tiny cracks develop into larger failures.

Bridging originates from a matrix rupture and a fiber pull-out, as mentioned above. A crack in the matrix widens as much as the fiber is exposed outside without breakage. When this occurs, the fiber acts as a bridge between the separated parts of the matrix.

The strengths of the reinforcement and the matrix are quite different. For example, the ultimate strength of carbon fiber is 3.5 GPa, while that of polyester is 6.6 MPa, and the elastic modulus is 70 GPa and 243 MPa, respectively. These differences generate interlaminar shear stress, which is lateral shear stress between two laminars. This separates the laminars inside the boundary of the matrix, which has a relatively weak modulus and strength.[65] We call this “delamination.”

3.3.2 SHM in Elastic Regime

Since the late 1990s, CFRPs have been investigated by laminate theories. J. Xiao et al.[66] studied tensor and numerical analyses of CFRPs, and applied physical behavior to piezoresistivity.

S. Wang et al.[67] thoroughly investigated the piezoresistivity of

continuous unidirectional (UD) CFRPs under cyclic tensile tests. They compared the results of the four-probe method and the two-probe method, and measured the composite piezoresistivity and the contact resistance, respectively. Furthermore, the piezoresistivity of UD CFRPs decreased with tensile loading owing to the increased degree of fiber alignment.

S. Wang et al.[68] conducted several tests on temperature, humidity, mechanical stress, and mechanical strain. Analyzing the piezoresistivity of a carbon-fiber interlaminar interface under different conditions of temperature, humidity, mechanical strain, and stress, the researchers determined the self-sensing capability of a CFRP. The uniqueness of this paper is its consideration of interlaminar behaviors of the piezoresistive material. Moreover, *in-situ* self-sensing CFRPs were widely investigated under various conditions.[68-71]

J. Abry et al.[70] studied UD CFRPs with different methods such as four-probe and two-probe measurements. This paper dealt with a self-sensing mechanism beyond the elastic region, so that damage to the composite could be also detected.

A. Todoroki et al.[72,73] carried out a structural numerical analysis of CFRPs and related it to changes in electrical resistance. As shown in Fig. 5, the piezoresistive results of CFRPs are represented with respect to the different loading and the different measuring directions in their papers. This anisometric piezoresistivity analysis was applied into laminate theory and FEM (Finite Element Method) analysis in 2011.[74]

He also showed interest in measuring mechanisms. He and J. Yoshida[75] researched electrode connections. The electrical resistance change in a single-ply CFRP was investigated by comparing the electrode connection conditions. The researchers concluded that a poor electrode connection leads to negative piezoresistivity owing to electrical contact damage. Further study about poor contact between the composite and the electrodes was conducted via FEM analysis.

3.3.3 Beyond Fracture

J. Abry et al.[76] investigated the composite failure process by observing the resistance in 1999. In the experiment, electrical resistance appeared when a failure occurred. J. Park et al. and Z. Xia et al.[77,78] proposed an electrical-resistance equivalent model of CFRPs. They stated that a fracture in the composite is equal to a short in the electrical network, as depicted in Fig. 6.

A. Todoroki et al.[79] utilized the orthotropic electric conductance of CFRP laminates to detect delamination. In this paper, electrical conductance was measured using different fiber volume fraction laminates. In addition, electrical resistance differences in pure and cracked samples were compared by FEM as well as experimental data. Analyzing the electrical current flow of the CFRPs by FEM, the researchers could identify the segment where delamination was inherent. The authors mentioned that this sensing is equal to using artificial neural networks.

From a theoretical viewpoint, M. S. Cham Prasad et al.[80] applied fracture mechanics to FRPs. The fracture mechanics were numerically combined with electrical resistance by A. Todoroki et al.,[81] who found a relationship between the piezoresistance and the mechanical strain under an elastic region. They compared the consensus between the electrical resistance and the load when there is a failure. Throughout these steps, the electrical current density in the through-thickness direction was also investigated by FEM.

Other types of SHM for CFRP have been investigated. For example, CFRP dents were discussed in another paper by A. Todoroki et al.,[82] who examined the electrical resistance of an artificial indentation in a CFRP. In addition, based on observations of electrical resistance, the effects of the number of electrodes were investigated by A. Todoroki[83] and Z. Xia et al..[78]

Recently, A. Todoroki et al.[84] adopted a new method for a CFRP self-sensing method. They measured the voltage of copper tapes impregnated in a CFRP. When there is a failure, the input voltage is distorted in real time. The time domain reflectometry (TDR) method and curved microstrip line (MSL) method measure the time-domain pulse-transmission signal in small channels. Even though defects far from the copper line as they cannot be detected, fiber breakage near the line can be monitored for short periods when the wave velocity is more than 10^8 m/s.

With regard to the delamination rate, M. J. Donough[85] examined the effects of the loading rate when CFRPs were undergoing fatigue tests. He compared the endurance life with different fatigue loading rates, and analyzed the fiber bridging law by experiments. The results were verified by the strain energy rate as well as the fracture energy.

3.4 Modeling of CFRPs for SHM

Both macro- and microscale CFRP monitoring can be investigated by computational analysis.[86-88] The main advantage of a simulation is that unseen phenomena such as stress and electrical current density can be visualized.

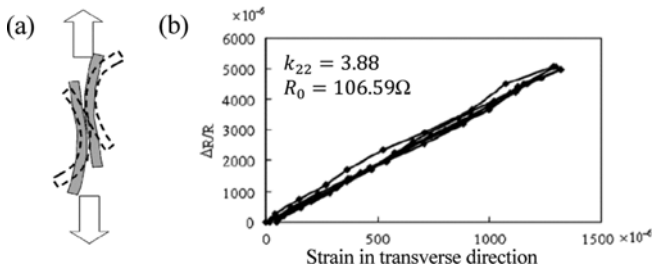

Fig. 5 (a) Fiber alignment during tensile loading, (b) Positive piezoresistivity during the tensile loading both from[73] (Adapted from Ref. 73 with Permission)

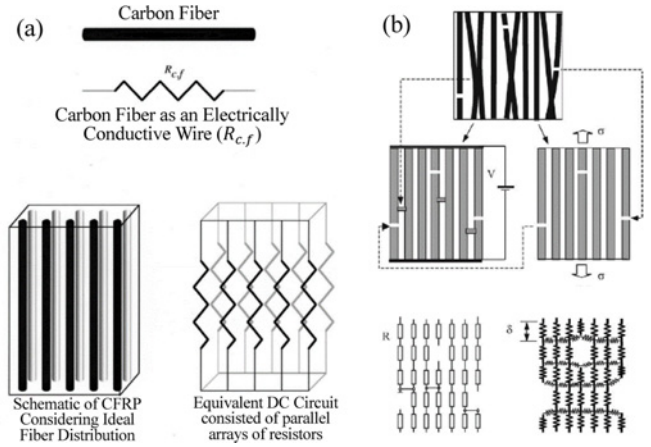

Fig. 6 Electrical-Resistance equivalent models of CFRPs extracted from (a)[77] and (b)[78] (Adapted from Ref. 77, 78 with Permission)

3.4.1 Mechanical Failure Modeling by FEM

Because the general failure in FRPs is delamination, A. Todoroki et al.[83] and R. Schueler et al.[89] solved the inverse problem of detecting the size and location of a delamination by using an artificial neural network and response surfaces method.[90] As shown in Fig. 7, the input layer is the electrical resistance ratio, and the output layer is the normalized delamination size (a/L) and location (p/L). An artificial neural network is usually used when there are complex algorithms with numerous inputs and outputs. In this context, with the aid of FEM, the number of electrodes can be compromised, and at the same time failures can be detected by measured the electrical resistance.

3.4.2 Current Distribution and Electrical Resistance Modeling

A. Todoroki et al.[79] used FEM analysis to investigate the effects of orthotropic electrical conductivity during delamination monitoring. They adopted an ANSYS auto mesh generation system for the analysis. They measured the voltage change distribution according to the fiber volume fraction when the delamination was located between electrodes, and plotted a contour plot of electric voltage from FEM. As shown in Fig. 8, the electrical current density is gradual in the thickness direction at Fig. 8(a), but Fig. 8(b) shows the horizontal electric current flow. Because of the gradual electric current in the thickness direction, detecting a delamination crack between electrodes with a resistance change is feasible. This is shown in the upper schematic of Fig. 8(b).

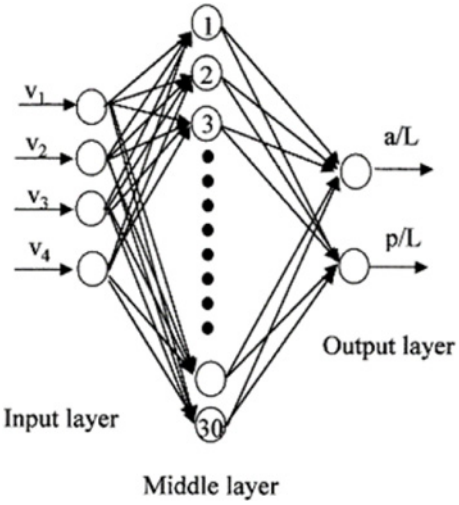

Fig. 7 Artificial neural network structure from[83] (Adapted from Ref. 83 with Permission)

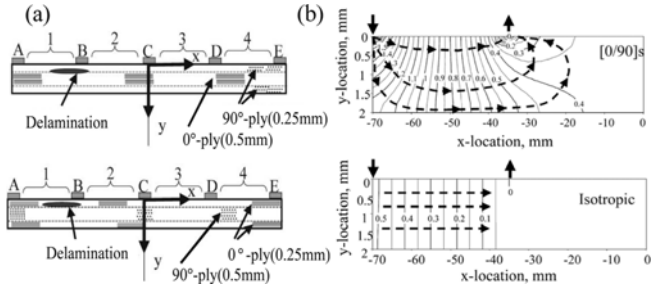

Fig. 8 Specimen configurations for delamination monitoring: (a) Laminate of $[0/90]_s$ and laminate of $[90/0]_s$, (b) Contour plot of electric voltage from[79] (Adapted from Ref. 79 with Permission)

However, if the electric current flows horizontally in a laminate composite, as shown in the lower schematic of Fig. 8(b), detecting the delamination within the composite is difficult because the change in resistance of the delamination is undetectably small. A similar study with similar results was reported by M. Louis.[91]

N. Angelidis et al.[92] and A. Todoroki[93] further analyzed the electrical current density vector by FEM studies. Fig. 9(a) shows the electrical current density vector in a cross-sectional view. As indicated by the circle in the figure, the electrical current flows in the thickness direction and in the second ply. Current continues to flow until it reaches the electrode, as shown in Fig. 9(b).

In addition, A. Todoroki[74] analyzed the electrical current within a thick laminated CFRP composite. This study supports the conclusion that thin-CFRP-plate theory cannot be applied to a thick CFRP composite.[94,95] This is because the voltage difference in a thin CFRP composite is uniform in the thickness direction, while that of

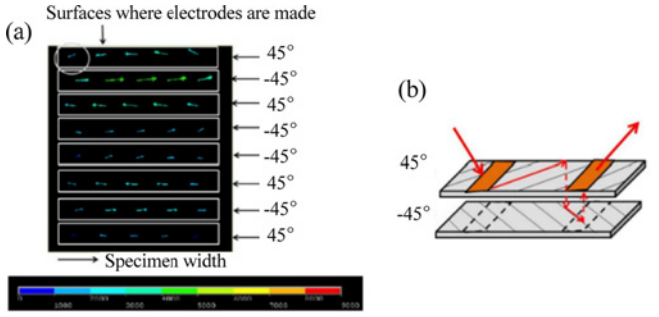

Fig. 9 (a) Electrical current density vectors of cross section, (b) Schema of electric current of +-45 CFRP laminate from[93] (Adapted from Ref. 93 on the basis of OA)

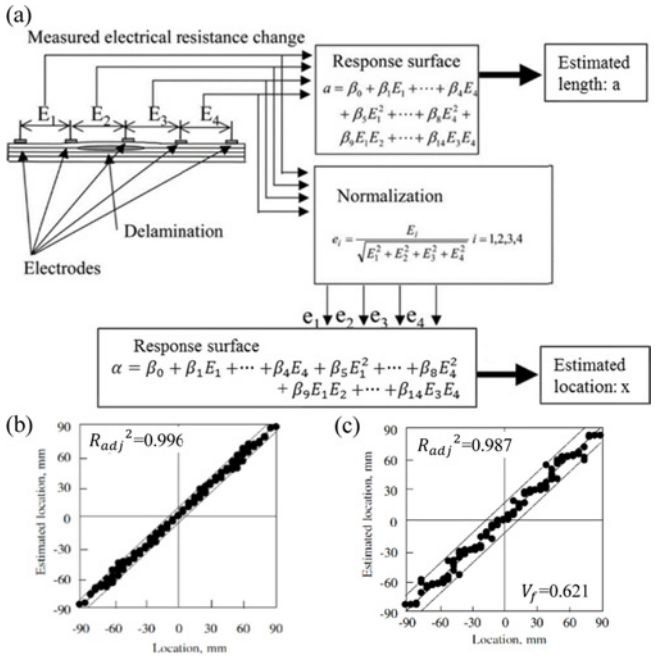

Fig. 10 (a) Algorithm for analyzing electrical resistance change generated from delamination, (b) and (c) Comparison of FEM and experimental results of delamination in terms of different fiber volume fractions from[95] (Adapted from Ref. 95 with Permission)

a thick CFRP composite decreases with farther distance from the charged surface.

A. Todoroki et al.[95] proposed a delamination monitoring system and verified that the suggested analytical and experimental results fit each other with small deviations, as shown in Fig. 10. Furthermore, they investigated the relevance between electrode spacing and delamination monitoring performance for both high- and low-fiber-volume fraction laminates.

3.4.3 Electromechanical Modeling

D. D. L. Chung et al.[67,96] reported on changes in resistance for a unidirectional CFRP under tensile loading owing to fiber re-alignment. Moreover, A. Todoroki et al.[73] developed an analytical model for resistance changes in a misaligned ply model. This paper explained the negative resistance changes that occurred when the unidirectional CFRP had a tensile load along the fiber direction.

J. Park et al.[77] examined the relationship between CFRP failure and electrical resistance under tensile loading. Because the carbon fiber dominates the electrical properties of a CFRP, the electrical resistance changed abruptly if the carbon fiber was detached from the adjacent fiber or damaged. The authors used a GLS (Global Load Sharing) assumption to evaluate the mechanical damage.[97] In addition, a CFRP composite can be converted into an electrical circuit model, as shown in Fig. 6.

However, to consider the fiber contacts, a new concept was proposed: electrical ineffective length.[98] The authors found the relation between the change in resistance of a proposed DC circuit and the electrical ineffective length. Eq. (1) represents the resistance change of the DC circuit under tensile loading, which is affected by the ineffective length:

$$\frac{\Delta R_T}{R_{T0}} = (1+\alpha\varepsilon)\exp\left[\left(\frac{\gamma_T\beta\delta_{ec}}{\delta_c}\right)\left(\frac{E_f\varepsilon}{\sigma_c}\right)^m\right]-1;$$
$$\frac{\Delta R_L}{R_{L0}} = (1+\alpha\varepsilon)\exp\left[\left(\frac{\gamma_L\beta\delta_{ec}}{\delta_c}\right)\left(\frac{E_f\varepsilon}{\sigma_c}\right)^m\right]-1; \quad (1)$$

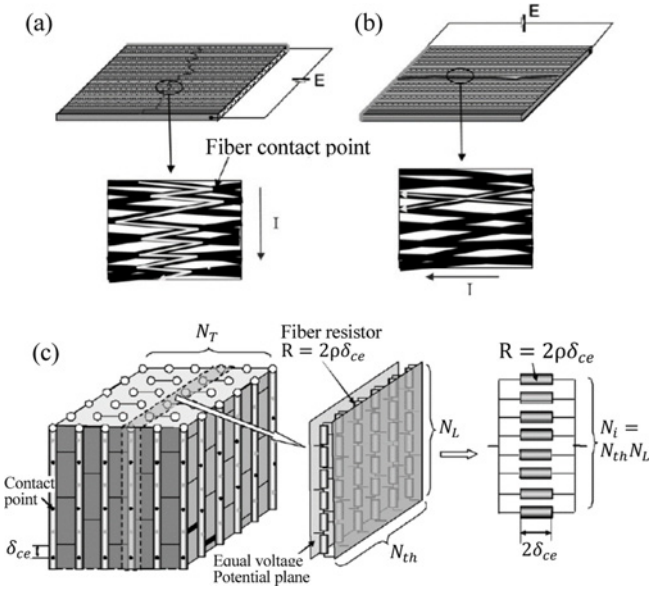

Fig. 11 Schematic representations of electrical path in a CFRP in (a) Transverse and (b) Longitudinal directions (c) Three-Dimensional equivalent electrical resistance model of a CFRP, extracted from[100] (Adapted from Ref. 100 with Permission)

where $\Delta R/R_0$ is the normalized resistance change, α is the gage factor of carbon fiber, ε is the applied strain, β is the geometry factor, γ is the additional fitting factor, E_f is Young's modulus of the carbon fiber, and m and σ_0 are the Weibull shape and scale parameters, respectively, corresponding to reference length L_0.

In addition, the authors applied the electrical ineffective length to a Monte Carlo simulation by assuming that the electrical nodes are located at the same locations within the fiber, although they are randomly distributed. Moreover, the fiber length is proportional to the possibility of a fiber breakage, according to Weibull-Poisson statistics.[99]

Similar research was conducted by Z. Xia et al..[100] Fig. 11 shows the representative schematics of their study. Assuming the contact points of the carbon fiber are electrical paths, a three-dimensional electrical-resistance equivalent circuit of the CFRP was established by assembling the 1-dimensional, 2-dimensional, and 3-dimensional elements in sequence, as shown in Fig. 11(c).

4. Conclusions

As the usage of carbon-material-reinforced or filled polymers is constantly increasing, SHM is becoming more and more important to ensure their structural integrity and safety. Carbon material/polymer composites unique smart characteristics, such as in-situ self-sensing based on piezoresistive effects. Regardless of the length scale of reinforcement, such as CNT, graphene, and carbon fiber, mechanical strains and physical failures can be monitored by observing the electrical resistance measured from the conductive carbon material network of the structure. In addition, physical monitoring can be combined with the equivalent electrical network model of carbon material/polymer composites to predict deformations and failures. Refined models, electrode placement schemes, and algorithms to correlated electrical resistance and structural state are necessary and promising areas for future research for SHM of large structures.

ACKNOWLEDGMENTS

This research was supported by the Basic Science Research Program (Mid-Career Research Program) through the National Research Foundation funded by the Ministry of Science, ICT and Future Planning, Korea (Grant No. 2016R1A2B4015335) and the 2016 Research Fund (1.160005.01) of UNIST (Ulsan National Institute of Science and Technology).

REFERENCES

1. Hwang, W.-C., Yang, Y.-J., Cha, C.-S., Jung, J.-A., Kim, J.-H., et al., "Impact Collapse Behavior of CFRP Structural Members according to the Variation of Section Shapes and Stacking Angles," Int. J. Precis. Eng. Manuf., Vol. 16, No. 4, pp. 677-684, 2015.
2. Shahrajabian, H. and Farahnakian, M., "Modeling and Multi-Constrained Optimization in Drilling Process of Carbon Fiber

Reinforced Epoxy Composite," Int. J. Precis. Eng. Manuf., Vol. 14, No. 10, pp. 1829-1837, 2013.

3. Hong, S. W., Ahn, S. S., Li, H., Kim, J. K., Sang, J. K., et al., "Charpy Impact Fracture Characteristics of CFRP Composite Materials According to Variations of Fiber Array Direction and Temperature," Int. J. Precis. Eng. Manuf., Vol. 14, No. 2, pp. 253-258, 2013.
4. Ahn, S. S., Hong, S. W., Koo, J. M., and Seok, C. S., "Prediction of Compressive Strength of CFRP Composite Structures Using Notch Strength," Int. J. Precis. Eng. Manuf., Vol. 14, No. 6, pp. 1103-1108, 2013.
5. Jeon, K.-W., Shin, K.-B., and Kim, J.-S., "Evaluation of Tension-Compression and Tension-Tension Fatigue Life of Woven Fabric Glass/Epoxy Laminate Composites Used in Railway Vehicle," Int. J. Precis. Eng. Manuf., Vol. 12, No. 5, pp. 813-820, 2011.
6. Tsao, C. C. and Hocheng, H., "Computerized Tomography and C-Scan for Measuring Delamination in the Drilling of Composite Materials Using Various Drills," International Journal of Machine Tools and Manufacture, Vol. 45, No. 11, pp. 1282-1287, 2005.
7. Gros, X. E., Ogi, K., and Takahashi, K., "Eddy Current, Ultrasonic C-Scan and Scanning Acoustic Microscopy Testing of Delaminated Quasi-Isotropic CFRP Materials: A Case Study," Journal of Reinforced Plastics and Composites, Vol. 17, No. 5, pp. 389-405, 1998.
8. Mook, G., Pohl, J., Michel, F., and Benziger, T., "Damage Evaluation of Smart CFRP-Piezoceramic-Materials Using Non-Destructive Methods," Proc. of ICCM-12 Conference on Composite Materials Paris, pp. 1-10, 1999.
9. Lane, R. A., "Sensors and Sensing Technologies for Integrated Vehicle Health Monitoring Systems," pp. 11-15, 2004.
10. Wang, P., Tamilselvan, P., Twomey, J., and Youn, B. D., "Prognosis-Informed Wind Farm Operation and Maintenance for Concurrent Economic and Environmental Benefits," Int. J. Precis. Eng. Manuf., Vol. 14, No. 6, pp. 1049-1056, 2013.
11. Lange, R. and Mook, G., "Structural Analysis of CFRP Using Eddy Current Methods," NDT & E International, Vol. 27, No. 5, pp. 241-248, 1994.
12. Riegert, G., Zweschper, T., and Busse, G., "Lockin Thermography with Eddy Current Excitation," Quantitative InfraRed Thermography Journal, Vol. 1, No. 1, pp. 21-32, 2004.
13. Schulze, M. H., Heuer, H., Küttner, M., and Meyendorf, N., "High-Resolution Eddy Current Sensor System for Quality Assessment of Carbon Fiber Materials," Microsystem Technologies, Vol. 16, No. 5, pp. 791-797, 2010.
14. Yin, W., Withers, P. J., Sharma, U., and Peyton, A. J., "Noncontact Characterization of Carbon-Fiber-Reinforced Plastics Using Multifrequency Eddy Current Sensors," IEEE Transactions on Instrumentation and Measurement, Vol. 58, No. 3, pp. 738-743, 2009.
15. Lee, J., Sheen, B., and Cho, Y., "Quantitative Tomographic Visualization for Irregular Shape Defects by Guided Wave Long Range Inspection," Int. J. Precis. Eng. Manuf., Vol. 16, No. 9, pp. 1949-1954, 2015.
16. Seo, H., Jhang, K.-Y., Kim, K.-C., and Hong, D.-P., "Improvement of Crack Sizing Performance by Using Nonlinear Ultrasonic Technique," Int. J. Precis. Eng. Manuf., Vol. 15, No. 11, pp. 2461-2464, 2014.
17. Park, J.-W., Im, K.-H., Yang, I.-Y., Kim, S.-K., Kang, S.-J., et al. "Terahertz Radiation NDE of Composite Materials for Wind Turbine Applications," Int. J. Precis. Eng. Manuf., Vol. 15, No. 6, pp. 1247-1254, 2014.
18. Im, K.-H., Lee, K.-S., Yang, I.-Y., Yang, Y.-J., Seo, Y.-H., et al. "Advanced T-Ray Nondestructive Evaluation of Defects in FRP Solid Composites," Int. J. Precis. Eng. Manuf., Vol. 14, No. 6, pp. 1093-1098, 2013.
19. Kim, G., Hong, S., Jhang, K.-Y., and Kim, G. H., "NDE of Low-Velocity Impact Damages in Composite Laminates Using ESPI, Digital Shearography and Ultrasound C-Scan Techniques," Int. J. Precis. Eng. Manuf., Vol. 13, No. 6, pp. 869-876, 2012.
20. Hsu, D. K., Lee, K.-S., Park, J.-W., Woo, Y.-D., Im, K. H., "NDE Inspection of Terahertz Waves in Wind Turbine Composites," Int. J. Precis. Eng. Manuf., Vol. 13, No. 7, pp. 1183-1189, 2012.
21. Gao, D., Wang, Y., Wu, Z., Rahim, G., and Ba, S., "Design of a Sensor Network for Structural Health Monitoring of a Full-Scale Composite Horizontal Tail," Smart Materials and Structures, Vol. 23, No. 5, 2014.
22. Tsao, C., "Thrust Force and Delamination of Core-Saw Drill during Drilling of Carbon Fiber Reinforced Plastics (CFRP)," The International Journal of Advanced Manufacturing Technology, Vol. 37, No. 1-2, pp. 23-28, 2008.
23. Soutis, C. and Curtis, P., "Prediction of the Post-Impact Compressive Strength of CFRP Laminated Composites," Composites Science and Technology, Vol. 56, No. 6, pp. 677-684, 1996.
24. Tsao, C. and Hocheng, H., "Computerized Tomography and C-Scan for Measuring Delamination in the Drilling of Composite Materials Using Various Drills," International Journal of Machine Tools and Manufacture, Vol. 45, No. 11, pp. 1282-1287, 2005.
25. Quaegebeur, N., Micheau, P., Masson, P., and Maslouhi, A., "Structural Health Monitoring Strategy for Detection of Interlaminar Delamination in Composite Plates," Smart Structures and Materials, Vol. 19, No. 8, 2011.
26. Diamanti, K. and Soutis, C., "Structural Health Monitoring Techniques for Aircraft Composite Structures," Progress in Aerospace Sciences, Vol. 46, No. 8, pp. 342-352, 2010.
27. Shmaliy, Y. S., Ibarra-Manzano, O., Aridrade-Lucio, J., and Rojas-Laguna, R., "Approximate Estimates of Limiting Errors of Passive Wireless Saw Sensing with DPM," IEEE Transactions on

Ultrasonics, Ferroelectrics, and Frequency Control, Vol. 52, No. 10, pp. 1797-1805, 2005.

28. Singh, R. K. and Chennamsetti, R., "Propagation of Ao Mode through the Front Edge of a Delamination: Numerical and Experimental Studies," Int. J. Precis. Eng. Manuf., Vol. 15, No. 8, pp. 1639-1645, 2014.
29. Jeong, H., Lee, J.-S., and Bae, S.-M., "Defect Detection and Localization in Plates Using a Lamb Wave Time Reversal Technique," Int. J. Precis. Eng. Manuf., Vol. 12, No. 3, pp. 427-434, 2011.
30. Kang, D., Kim, H.-Y., Kim, D.-H., and Park, S., "Thermal Characteristics of FBG Sensors at Cryogenic Temperatures for Structural Health Monitoring," Int. J. Precis. Eng. Manuf., Vol. 17, No. 1, pp. 5-9, 2016.
31. Kim, C., Kim, K., Kim, H., Paek, I., Yoo, N., et al. "A Method to Estimate Bending Moments Acting on a Wind Turbine Blade Specimen Using FBG Sensors," Int. J. Precis. Eng. Manuf., Vol. 13, No. 7, pp. 1247-1250, 2012.
32. Bang, H.-J., Kim, H.-I., and Lee, K.-S., "Measurement of Strain and Bending Deflection of a Wind Turbine Tower Using Arrayed FBG Sensors," Int. J. Precis. Eng. Manuf., Vol. 13, No. 12, pp. 2121-2126, 2012.
33. Chan, T. H., Yu, L., Tam, H. Y., Ni, Y. Q., Liu, S. Y., et al., "Fiber Bragg Grating Sensors for Structural Health Monitoring of Tsing Ma Bridge: Background and Experimental Observation," Engineering Structures, Vol. 28, No. 5, pp. 648-659, 2006.
34. Takeda, S., Minakuchi, S., Okabe, Y., and Takeda, N., "Delamination Monitoring of Laminated Composites Subjected to Low-Velocity Impact Using Small-Diameter FBG Sensors," Composites Part A: Applied Science and Manufacturing, Vol. 36, No. 7, pp. 903-908, 2005.
35. Botsev, Y., Arad, E., Tur, M., Kressel, I., Ben-Sinon, U., et al. "Damage Detection under a Composite Patch Using an Embedded PZT-FBG Ultrasonic Sensor Array," Proc. of 3rd European Workshop on International Society for Optics and Photonics, Vol. 6619, 2007.
36. Minakuchi, S., Banshoya, H., Ii, S., and Takeda, N., "Hierarchical Fiber-Optic Delamination Detection System for Carbon Fiber Reinforced Plastic Structures," Smart Materials and Structures, Vol. 21, No. 10, 2012.
37. Davis, C. E., Norman, P., Ratcliffe, C., and Crane, R., "Broad Area Damage Detection in Composites Using Fibre Bragg Grating Arrays," Structural Health Monitoring, Vol. 11, No. 6, pp. 724-732, 2012.
38. Davis, C., Baker, W., Moss, S. D., Galea, S. C., and Jones, R., "In Situ Health Monitoring of Bonded Composite Repairs Using a Novel Fiber Bragg Grating Sensing Arrangement," Proc. of International Society for Optics and Photonics of International Symposium on Smart Materials, Nano-, Micro-Smart Systems, pp. 140-149, 2002.
39. Kalinin, V., "Wireless Physical Saw Sensors for Automotive Applications," Proc. of 2011 IEEE International Ultrasonics Symposium, pp. 212-221, 2011.
40. Jang, S., Jo, H., Cho, S., Mechitov, K., Rice, J. A., et al., "Structural Health Monitoring of a Cable-Stayed Bridge Using Smart Sensor Technology: Deployment and Evaluation," Smart Structures and Systems, Vol. 6, No. 5-6, pp. 439-459, 2010.
41. Qiu, L. and Yuan, S., "On Development of a Multi-Channel PZT Array Scanning System and Its Evaluating Application on UAV Wing Box," Sensors and Actuators A: Physical, Vol. 151, No. 2, pp. 220-230, 2009.
42. Jeong, M., Bae, J.-G., and Koh, B.-H., "A Feasibility Study of Damage Tracking through the Diffusive Communication of Wireless Sensors," Int. J. Precis. Eng. Manuf., Vol. 11, No. 1, pp. 23-29, 2010.
43. Fan, Y. and Kahrizi, M., "Characterization of a FBG Strain Gage Array Embedded in Composite Structure," Sensors and Actuators A: Physical, Vol. 121, No. 2, pp. 297-305, 2005.
44. Ciampa, F. and Meo, M., "A New Algorithm for Acoustic Emission Localization and Flexural Group Velocity Determination in Anisotropic Structures," Composites Part A: Applied Science and Manufacturing, Vol. 41, No. 12, pp. 1777-1786, 2010.
45. Geim, A. K. and Novoselov, K. S., "The Rise of Graphene," Nature Materials, Vol. 6, No. 3, pp. 183-191, 2007.
46. Ashby, M., Gibson, L., Wegst, U., and Olive, R., "The Mechanical Properties of Natural Materials. I. Material Property Charts," Proc. of the Royal Society of Physical and Engineering Sciences, pp. 123-140, 1995.
47. Shin, Y. C., Novin, E., and Kim, H., "Electrical and Thermal Conductivities of Carbon Fiber Composites with High Concentrations of Carbon Nanotubes," Int. J. Precis. Eng. Manuf., Vol. 16, No. 3, pp. 465-470, 2015.
48. Yoo, L. and Kim, H., "Conductivities of Graphite Fiber Composites with Single-Walled Carbon Nanotube Layers," Int. J. Precis. Eng. Manuf., Vol. 12, No. 4, pp. 745-748, 2011.
49. Wang, X. and Chung, D., "Short-Carbon-Fiber-Reinforced Epoxy as a Piezoresistive Strain Sensor," Smart Materials and Structures, Vol. 4, No. 4, pp. 363, 1995.
50. Chung, D., "Cement Reinforced with Short Carbon Fibers: A Multifunctional Material," Composites Part B: Engineering, Vol. 31, No. 6, pp. 511-526, 2000.
51. Chung, D., "Piezoresistive Cement-Based Materials for Strain Sensing," Journal of Intelligent Material Systems and Structures, Vol. 13, No. 9, pp. 599-609, 2002.
52. Wang, X., Fu, X., and Chung, D. D., "Piezoresistive Strain Sensors in the Form of Short Carbon Fiber Composites," Proc. of 5th Smart Structures and Materials, International Society for Optics and Photonics, Vol. 3324, pp. 115-126, 1998.

53. Chung, D., "Cement-Matrix Composites for Smart Structures," Smart Materials and Structures, Vol. 9, No. 4, pp. 389-401, 2000.

54. Wen, S. and Chung, D., "Pitch-Matrix Composites for Electrical, Electromagnetic and Strain-Sensing Applications," Journal of Materials Science, Vol. 40, No. 15, pp. 3897-3903, 2005.

55. Park, J.-M., Kim, P.-G., Jang, J.-H., Wang, Z., Kim, J.-W., et al., "Self-Sensing and Dispersive Evaluation of Single Carbon Fiber/ Carbon Nanotube (CNT)-Epoxy Composites Using Electro-Micromechanical Technique and Nondestructive Acoustic Emission," Composites Part B: Engineering, Vol. 39, No. 7, pp. 1170-1182, 2008.

56. Hu, N., Fukunaga, H., Atobe, S., Liu, Y., and Li, J., "Piezoresistive Strain Sensors Made from Carbon Nanotubes Based Polymer Nanocomposites," Sensors, Vol. 11, No. 11, 2011.

57. Kang, I., Schulz, M. J., Kim, J. H., Shanov, V., and Shi, D., "A Carbon Nanotube Strain Sensor for Structural Health Monitoring," Smart Materials and Structures, Vol. 15, No. 3, pp. 737-748, 2006.

58. Todoroki, A. and Tanaka, Y., "Delamination Identification of Cross-Ply Graphite/Epoxy Composite Beams Using Electric Resistance Change Method," Composites Science and Technology, Vol. 62, No. 5, pp. 629-639, 2002.

59. Feraboli, P., Cleveland, T., Ciccu, M., Stickler, P., and De Oto, L., "Defect and Damage Analysis of Advanced Discontinuous Carbon/ Epoxy Composite Materials," Composites Part A: Applied Science and Manufacturing, Vol. 41, No. 7, pp. 888-901, 2010.

60. Ku-Herrera, J. and Aviles, F., "Cyclic Tension and Compression Piezoresistivity of Carbon Nanotube/Vinyl Ester Composites in the Elastic and Plastic Regimes," Carbon, Vol. 50, No. 7, pp. 2592-2598, 2012.

61. Böger, L., Wichmann, M. H., Meyer, L. O., and Schulte, K., "Load and Health Monitoring in Glass Fibre Reinforced Composites with an Electrically Conductive Nanocomposite Epoxy Matrix," Composites Science and Technology, Vol. 68, No. 7, pp. 1886-1894, 2008.

62. Alexopoulos, N., Bartholome, C., Poulin, P., and Marioli-Riga, Z., "Structural Health Monitoring of Glass Fiber Reinforced Composites Using Embedded Carbon Nanotube (CNT) Fibers," Composites Science and Technology, Vol. 70, No. 2, pp. 260-271, 2010.

63. Vavouliotis, A., Paipetis, A., and Kostopoulos, V., "On the Fatigue Life Prediction of CFRP Laminates Using the Electrical Resistance Change Method," Composites Science and Technology, Vol. 71, No. 5, pp. 630-642, 2011.

64. Abot, J. L., Song, Y., Vatsavaya, M. S., Medikonda, S., Kier, Z., et al. "Delamination Detection with Carbon Nanotube Thread in Self-Sensing Composite Materials," Composites Science and Technology, Vol. 70, No. 7, pp. 1113-1119, 2010.

65. Kim, S.-C., Kim, J. S., and Yoon, H.-J., "Experimental and Numerical Investigations of Mode I Delamination Behaviors of Woven Fabric Composites with Carbon, Kevlar and Their Hybrid Fibers," Int. J. Precis. Eng. Manuf., Vol. 12, No. 2, pp. 321-329, 2011.

66. Xiao, J., Li, Y., and Fan, W., "A Laminate Theory of Piezoresistance for Composite Laminates," Composites Science and Technology, Vol. 59, No. 9, pp. 1369-1373, 1999.

67. Wang, S. and Chung, D., "Piezoresistivity in Continuous Carbon Fiber Polymer-Matrix Composite," Polymer Composites, Vol. 21, No. 1, pp. 13-19, 2000.

68. Wang, S., Kowalik, D. P., and Chung, D., "Self-Sensing Attained in Carbon-Fiber-Polymer-Matrix Structural Composites by Using the Interlaminar Interface as a Sensor," Smart Materials and Structures, Vol. 13, No. 3, pp. 570-592, 2004.

69. Takeda, T., Shindo, Y., Fukuzaki, T., and Narita, F., "Short Beam Interlaminar Shear Behavior and Electrical Resistance-Based Damage Self-Sensing of Woven Carbon/Epoxy Composite Laminates in a Cryogenic Environment," Journal of Composite Materials, pp. 1-10, 2012.

70. Abry, J., Choi, Y., Chateauminois, A., Dalloz, B., Giraud, G., et al. "In-Situ Monitoring of Damage in CFRP Laminates by Means of AC and DC Measurements," Composites Science and Technology, Vol. 61, No. 6, pp. 855-864, 2001.

71. Song, D.-Y., Takeda, N., and Kitano, A., "Correlation between Mechanical Damage Behavior and Electrical Resistance Change in CFRP Composites as a Health Monitoring Sensor," Materials Science and Engineering: A, Vol. 456, No. 1, pp. 286-291, 2007.

72. Todoroki, A. and Yoshida, J., "Electrical Resistance Change of Unidirectional CFRP Due to Applied Load," Japan Society of Mechanical Engineers International Journal Series A, Vol. 47, No. 3, pp. 357-364, 2004.

73. Todoroki, A., Samejima, Y., Hirano, Y., and Matsuzaki, R., "Piezoresistivity of Unidirectional Carbon/Epoxy Composites for Multiaxial Loading," Composites Science and Technology, Vol. 69, No. 11, pp. 1841-1846, 2009.

74. Todoroki, A., "Electric Current Analysis for Thick Laminated CFRP Composites," Transactions of the Japan Society for Aeronautical and Space Sciences, Vol. 55, No. 4, pp. 237-243, 2012.

75. Todoroki, A. and Yoshida, J., "Apparent Negative Piezoresistivity of Single-Ply CFRP due to Poor Electrical Contact of Four-Probe Method," Measurement, Vol. 1, pp. 1-6, 2005.

76. Abry, J., Bochard, S., Chateauminois, A., Salvia, M., and Giraud, G., "In Situ Detection of Damage in CFRP Laminates by Electrical Resistance Measurements," Composites Science and Technology, Vol. 59, No. 6, pp. 925-935, 1999.

77. Park, J., Okabe, T., Takeda, N., and Curtin, W., "Electromechanical Modeling of Unidirectional CFRP Composites under Tensile Loading Condition," Composites Part A: Applied Science and Manufacturing, Vol. 33, No. 2, pp. 267-275, 2002.

78. Xia, Z., Okabe, T., Park, J., Curtin, W., and Takeda, N., "Quantitative Damage Detection in CFRP Composites: Coupled Mechanical and Electrical Models," Composites Science and Technology, Vol. 63, No. 10, pp. 1411-1422, 2003.

79. Todoroki, A., Tanaka, M., and Shimamura, Y., "Measurement of Orthotropic Electric Conductance of CFRP Laminates and Analysis of the Effect on Delamination Monitoring with an Electric Resistance Change Method," Composites Science and Technology, Vol. 62, No. 5, pp. 619-628, 2002.

80. Prasad, M. S., Venkatesha, C., and Jayaraju, T., "Experimental Methods of Determining Fracture Toughness of Fiber Reinforced Polymer Composites under Various Loading Conditions," Journal of Minerals and Materials Characterization and Engineering, Vol. 10, No. 13, pp. 1263-1275, 2011.

81. Todoroki, A., Samejima, Y., Hirano, Y., Matsuzaki, R., and Mizutani, Y., "Mechanism of Electrical Resistance Change of a Thin CFRP Beam after Delamination Cracking," Journal of Solid Mechanics and Materials Engineering, Vol. 4, No. 1, pp. 1-11, 2010.

82. Todoroki, A., Shimazu, Y., and Misutani, Y., "Electrical Resistance Reduction of Laminated Carbon Fiber Reinforced Polymer by Dent Made by Indentation without Cracking," Journal of Solid Mechanics and Materials Engineering, Vol. 6, No. 12, pp. 1042-1052, 2012.

83. Todoroki, A. "The Effect of Number of Electrodes and Diagnostic Tool for Monitoring the Delamination of CFRP Laminates by Changes in Electrical Resistance," Composites Science and Technology, Vol. 61, No. 13, pp. 1871-1880, 2001.

84. Todoroki, A., Yamada, K., Mizutani, Y., Suzuki, Y., Matsuzaki, R., et al. "Self-Sensing Curved Micro-Strip Line Method for Damage Detection of CFRP Composites," Open Journal of Composite Materials, Vol. 4, No. 3, pp. , 2014.

85. Donough, M., Gunnion, A., Orifici, A., and Wang, C., "Scaling Parameter for Fatigue Delamination Growth in Composites under Varying Load Ratios," Composites Science and Technology, Vol. 120, pp. 39-48, 2015.

86. Ranjit, S., Kang, K., and Kim, W., "Investigation of Lock-in Infrared Thermography for Evaluation of Subsurface Defects Size and Depth," Int. J. Precis. Eng. Manuf., Vol. 16, No. 11, pp. 2255-2264, 2015.

87. Gao, T. and Cho, J.-U., "A Study on Damage and Penetration Behaviour of Carbon Fiber Reinforced Plastic Sandwich at Various Impacts," Int. J. Precis. Eng. Manuf., Vol. 16, No. 8, pp. 1845-1850, 2015.

88. Koo, J.-M., Choi, J.-H., and Seok, C.-S., "Prediction of Residual Strength after Impact of CFRP Composite Structures," Int. J. Precis. Eng. Manuf., Vol. 15, No. 7, pp. 1323-1329, 2014.

89. Schueler, R., Joshi, S. P., and Schulte, K., "Damage Detection in CFRP by Electrical Conductivity Mapping," Composites Science and Technology, Vol. 61, No. 6, pp. 921-930, 2001.

90. Gunst, R. F., "Response Surface Methodology: Process and Product Optimization Using Designed Experiments," Technometrics, Vol. 38, No. 3, pp. 284-286, 1996.

91. Louis, M., Joshi, S. P., and Brockmann, W., "An Experimental Investigation of Through-Thickness Electrical Resistivity of CFRP Laminates," Composites Science and Technology, Vol. 61, No. 6, pp. 911-919, 2001.

92. Angelidis, N., Khemiri, N., and Irving, P. E. "Experimental and Finite Element Study of the Electrical Potential Technique for Damage Detection in CFRP Laminates," Smart Materials and Structures, Vol. 14, No. 1, pp. 147-154, 2005.

93. Todoroki, A., Haruyama, D., Mizutani, Y., Suzuki, Y., and Yasuoka, T., "Electrical Resistance Change of Carbon/Epoxy Composite Laminates under Cyclic Loading under Damage Initiation Limit," Open Journal of Composite Materials, Vol. 4, No. 1, pp. 22-31, 2014.

94. Todoroki, A., "Electric Current Analysis of CFRP Using Perfect Fluid Potential Flow," Transactions of the Japan Society for Aeronautical and Space Sciences, Vol. 55, No. 3, pp. 183-190, 2012.

95. Todoroki, A., Tanaka, M., and Shimamura, Y., "Electrical Resistance Change Method for Monitoring Delaminations of CFRP Laminates: Effect of Spacing between Electrodes," Composites Science and Technology, Vol. 65, No. 1, pp. 37-46, 2005.

96. Wang, S. and Chung, D., "Negative Piezoresistivity in Continuous Carbon Fiber Epoxy-Matrix Composite," Journal of Materials Science, Vol. 42, No. 13, pp. 4987-4995, 2007.

97. Curtin, W., "Stochastic Damage Evolution and Failure in Fiber-Reinforced Composites," Advances in Applied Mechanics, Vol. 36, pp. 163-253, 1998.

98. Park, J. B., Okabe, T., and Takeda, N., "New Concept for Modeling the Electromechanical Behavior of Unidirectional Carbon-Fiber-Reinforced Plastic under Tensile Loading," Smart Materials and Structures, Vol. 12, No. 1, pp. 105-114, 2003.

99. Tsu, T., Mugele, R., and Mcclintock, F., "A Statistical Distribution Function of Wide Applicability," ASME-AMER Society Mechanical Engineering, pp. 233-234, 1952.

100. Xia, Z. and Curtin, W., "Modeling of Mechanical Damage Detection in CFRPs via Electrical Resistance," Composites Science and Technology, Vol. 67, No. 7, pp. 1518-1529, 2007.